PERFORMANCE OF AXIALLY COMPRESSED STIFFENED PANELS

SRINIVASAN SRIDHARAN and MAO-HUA PENG

Department of Civil Engineering, Washington University, Campus Box 1130, One Brookings Drive,
St. Louis, MO 63130, U.S.A.

Abstract—The paper reviews the theoretical foundations of a new analytical model developed for the study of nonlinear interaction of local and overall instabilities of axially compressed stiffened plates. It is shown that: the mixed second order field contains within itself all the essential secondary local modes liable to be triggered in the interaction; any such mode having an eigenvalue of the same order of magnitude as the primary local critical stress must be treated as a fundamental mode fully participating in the interaction in order that the analytical procedure is not riddled by singularities in the evaluation of the mixed second order field; and the technique of amplitude modulation is an effective substitute for accounting for a set of local modes of the same transverse description but of slightly differing wave lengths. The computational aspects are briefly touched upon and the form of an explicit potential energy function derived is shown.

The results obtained using the present model are then compared with the theoretical results obtained by Koiter and Pignataro and Tvergaard for several cases. The question of optimality is examined. The results confirm the earlier finding of Tvergaard that the optimally designed panels would have the local critical stresses higher than the overall buckling ones. A comparison of the present theory against the experimental results obtained by Thompson *et al.* for panels with "stocky" and "thin" stiffeners is then presented. In all cases, there is found to be very good agreement between the experimental and theoretical results.

NOTATION

Only the most important symbols are identified below

A	area of cross-section
E	Young's modulus of the material
P_L	lowest critical load
P_E	Euler critical load
U	axial displacement of the centroid of the section
W	lateral displacement of the member
W_1	lateral displacement as given by the overall buckling mode
b	width of the panel
d	depth of the stiffener
e	distance of the centroid of the stiffener from the middle surface of the plate
h	thickness of plate
h_0	averaged thickness of stiffened plate
k	buckling coefficient
m	the number of half-waves of local buckling
t_s	thickness of stiffener
u, v, w	the displacement components in x, y, z directions, respectively, caused by local buckling
$u_i, v_i, w_i \ (i > 1)$	the u, v, w displacements of the ith local mode
u_{ij}, v_{ij}, w_{ij}	second order displacements
w_0	the maximum out of plane imperfection in the shape of a local buckling mode
$\varepsilon_x, \varepsilon_y, \gamma_{xy}$	normal and shear strain components at the plate middle surface
v	Poisson's ratio
$\xi_i \ (i > 1)$	scaling factor associated with the ith mode
ξ_i^0	imperfection parameter (maximum displacement in the buckling mode/h, positive if inducing compression in the plate)
σ_0	the critical stress of plate of thickness h_0 without stiffeners
σ_1	overall critical stress
σ_2	lowest local critical stress
$\sigma_n \ (n > 2)$	critical stresses associated with secondary local modes
σ_{cr}	generic critical stress
χ	curvature of the overall deflection profile
$\chi_x, \chi_y, \chi_{xy}$	curvatures of plate elements in local buckling

INTRODUCTION

Stiffened plates find extensive applications in a variety of engineered structures. Their behavior under axial compression involves the nonlinear interaction between the local (plate) modes and overall (Euler) mode of buckling—a subject which has received con-

siderable attention in published literature (Tvergaard, 1973a; Koiter and Pignataro, 1976a; van der Neut, 1976). Any attempt at optimal design of these structural elements must be founded on an analytical model which is capable of describing the load–deformation characteristics with requisite accuracy and giving a reliable estimate of the maximum load carrying capacity.

The common notion that the optimal designs must be based on the concept of "simultaneous buckling" has been questioned by several investigators. It has been shown that such a design would be highly imperfection-sensitive and therefore may not remain optimal in presence of minute imperfections unavoidable in practice. Indeed Tvergaard (1973b) concluded that the optimum does indeed shift towards a range where the overall buckling stress (σ_1) is smaller than the local critical stress (σ_2).

In the analytical procedure outlined by Tvergaard (1973b), four modes were selected as being the most important ones. Apart from the primary local mode (designated as mode 2) corresponding to the lowest local critical stress and the overall mode (designated as mode 1), these were respectively a local mode having essentially the same transverse description as mode 2 but with a smaller half-wave length in the longitudinal direction, and a long-wave mode with its half-wave length equal to that of mode 1. These modes did appear to be the most important ones triggered in the interaction modes 1 and 2. However no detailed justification was offered for the choice nor a systematic technique outlined by which the important modes may be identified. We shall take up this point elsewhere in the paper.

Koiter and Pignataro (1976a) performed a detailed two-mode analysis of the "Tvergaard panel" (Tvergaard, 1973a) and established its imperfection-sensitivity. They used the technique of amplitude modulation by which the amplitude of the local mode was given freedom to vary. The case for the amplitude modulation was not argued by them, even though it is beginning to be realized as a real phenomenon.

For the case of Tvergaard panel which has shallow stocky stiffeners and equal values of the critical stresses $(\sigma_1 = \sigma_2)$, the analyses of Koiter and Tvergaard appear to be in broad agreement with each other. Koiter, however, realized that his analysis would not be applicable for plate structures with doubly symmetric sections as the key term $\xi_1 \xi_2^2$ (where ξ_1 and ξ_2 are the scaling parameters of modes 1 and 2, respectively) governing the interaction would vanish. For these cases, Koiter and Pignataro (1976b) recommend the inclusion of a key secondary local mode in the analysis. In fact Koiter and van der Neut pursue this idea for panels which have significant local buckling deformation on either side of the axis of overall bending in a subsequent paper (Koiter and van der Neut, 1980).

In the case of doubly symmetric sections, there exists a clear need for bringing to play a secondary local mode which should be antisymmetric with respect to the axis of overall bending, if the primary local mode were symmetric and vice versa. This follows simply upon an examination of the differential equation governing the mixed second order field, arising by an interaction of the modes 1 and 2 (Sridharan and Ali, 1985). Further, in order to accurately model its role, it must be taken as one of the fundamental modes participating in the interaction with the full complement of the higher order terms arising as a result, instead of letting it arise as a part of the second order field. This is because, in the latter case, its evaluation is riddled by the presence of a singularity in the equation giving the mixed second order field. The necessity of using amplitude modulated local modes for columns with doubly symmetric sections is also seen to follow from the same equation.

In the present paper, the mixed second order field equation is once again examined and a mathematical justification for the technique of "amplitude modulation" is put forward. It turns out that the technique is equivalent to considering several modes of the same transverse description but of differing wave lengths. It is shown that the mixed second order field, once solved for, provides the local basis for the choice of secondary local modes to be included as participating local modes in the analysis. Based on these concepts, a new beam element is developed, in which the relevant local buckling information is embedded. In contrast to the earlier work of Ali and Sridharan (1988) an explicit expression for the potential energy for the beam element is developed—a development which greatly facilitates computation and helps the clear perception of the mechanics of the interaction. The new beam element makes it possible to consider arbitrary end conditions for the stiffened panel.

The results produced by the present model are then compared with those of Koiter and Pignataro (1976b) and Tvergaard (1973b) and the experimental results of Thompson *et al.* (1976). The agreement is very satisfactory indeed. The present study confirms Tvergaard's conclusion that the optimal designs shift from the "naive optimum" (corresponding to coincident critical stresses) into the range where $\sigma_2/\sigma_1 > 1$, in the presence of imperfections. Of particular interest in the experimental study of Thompson *et al.* is the case of panel with slender stiffeners which exhibits a combined interaction of Euler buckling with respectively the "plate mode" and "stiffener mode" of local buckling. The latter is, however, of little importance for panels with stocky stiffeners.

THEORY

In this section, the theoretical basis of the analytical model is first established. This is followed by a description of the features of the beam element to be employed in the nonlinear analysis of the stiffened panel.

The following sequence is followed in developing the theory: the modelling of local buckling deformation is briefly reviewed; the derivation of the governing equation for the mixed second order field which arises by an interaction of a single local mode with overall bending is reviewed; the form of the solution to this equation is investigated; the source of singularities in the equation is identified; the necessity of taking more than one local mode as the fundamental mode participating in the interaction with the overall mode and allowing the amplitudes of the local modes to modulate, are then seen to follow as a logical consequences.

Description of local buckling deformation

The local buckling deformations are simply modelled using the "classical assumptions" suggested by Benthem (1959). These are:

(1) at a corner of the plate structure, where two plates meet at an angle, the normal displacement w for each plate vanishes;

(2) the normal stress resultant N_y in the transverse direction vanishes for each plate at the corner.

Thus the interaction of the constituent plates is solely in terms of the compatibility of rotations and inplane axial displacements at the plate junctions.

Given the foregoing assumptions, the following expressions for the mid-surface displacements u, v and w (Fig. 1) result from the von Karman theory of plates used in conjunction with the perturbation technique (Sridharan, 1982).
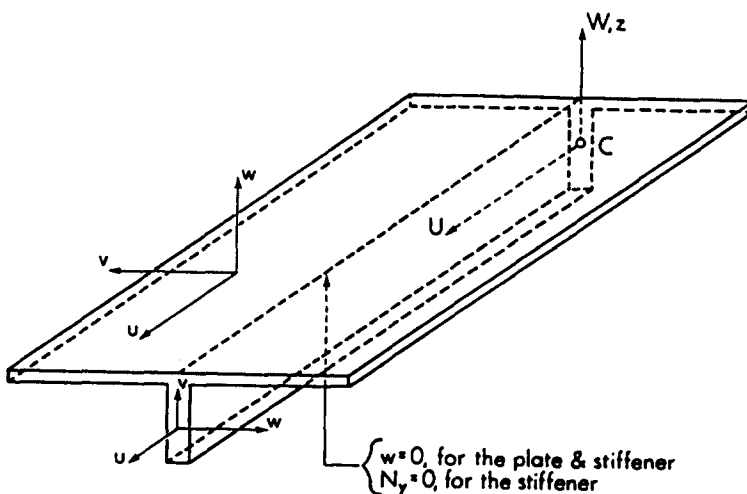

Fig. 1. The stiffened panel, the local coordinate system of the plate and stiffener (to describe local buckling deformation) and the global coordinate system (to describe overall bending deformations) (C = the centroid of the section).

First order fields $(\bar{u}_i)$:

$$u_i = v_i = 0$$

$$w_i = \bar{w}_i(y) \sin (m\pi x/l) \qquad (i = 2, \ldots, N, N+1). \tag{1a,b}$$

Second order fields $(\bar{u}_{ij})$:

$$u_{ij} = \bar{u}_{ij}(y) \sin (2m\pi x/l)$$

$$v_{ij} = \bar{v}_{0ij}(y) + \bar{v}_{2ij}(y) \cos (2m\pi x/l)$$

$$w_{ij} = 0 \qquad (i,j = 2, \ldots, N, N+1). \tag{2a--c}$$

In the foregoing, m represents for the number of half-waves of buckling, l the length of the structure. Note that single and double subscript refer respectively to the first and the second order quantities. The functions depending upon y, the transverse coordinate can be obtained for a prescribed uniform or linearly varying end shortening using the finite strip method (Graves-Smith and Sridharan, 1978; Sridharan, 1982). N is the number of local modes; and it would seem from eqn (2) that there are N^2 second order displacement fields. But since we can define $\bar{u}_{ij} = \bar{u}_{ji}$, there are only $N(N+1)/2$ independent second order fields.

The total mid-surface displacements in a purely local buckling problem, then take the form

$$u = u_0 + u_{ij}\,\xi_i\xi_j$$

$$v = v_0 + v_{ij}\,\xi_i\xi_j$$

$$w = w_i\xi_i \qquad (i,j = 1, \ldots, N) \tag{3a-c}$$

where u_0 and v_0 are the displacements due to prescribed end compression. For example, u_0 and v_0 are given by $\partial u_0/\partial x = -\lambda$, $\partial v_0/\partial y = v\lambda$ for the case of uniform end shortening, λl. For the case of prescribed end load, u_0 and v_0 would represent only the values corresponding to the unbuckled configuration and additional degrees of freedom representing the axial displacement at the centroid and the rotation of the entire section must be incorporated. Note that these degrees of freedom are also essential for the description of overall bending of the structure based on the conventional beam theory.

Appearance of the secondary modes and amplitude modulation

As the structure bends due to overall buckling, the local buckling deformation would be modified and, in general, can no longer be described in terms of a single mode. In particular, the deflections on the compression side of the neutral axis would be accentuated and those on the tension side reduced. In a two-mode interaction problem, this effect will be given by the mixed second order field.

In order to develop the equation giving this field, the membrane strain components (the normal strains ε_x and ε_y and the shearing strain γ_{xy}) are written in terms of the scalar parameters ξ_1 and ξ_2. Thus

$$
\left\{ \begin{array}{c} \varepsilon_x \\ \varepsilon_y \\ \gamma_{xy} \end{array} \right\}
= \left\{ \begin{array}{c} \varepsilon_{x_0} \\ \varepsilon_{y_0} \\ 0 \end{array} \right\}
+ \left\{ \begin{array}{c} \varepsilon_{x_1} \\ \varepsilon_{y_1} \\ \gamma_{xy_1} \end{array} \right\} \xi_1
+ \left\{ \begin{array}{c} \varepsilon_{x_2} \\ \varepsilon_{y_2} \\ \gamma_{xy_2} \end{array} \right\} \xi_2
+ \left\{ \begin{array}{c} \varepsilon_{x_{12}} \\ \varepsilon_{y_{12}} \\ \gamma_{xy_{12}} \end{array} \right\} \xi_1\xi_2 + \ldots \tag{4}
$$

The terms ε_{x_0} and ε_{y_0} are the strains corresponding to the unbuckled configuration. Equation (1a) gives $\varepsilon_{x_2} = \varepsilon_{y_2} = \gamma_{xy_2} = 0$. From the conventional beam theory $\varepsilon_{x_1} = -z\partial^2 W_1/\partial x^2$, $\varepsilon_{y_1} = -v\varepsilon_{x_1}$, $\gamma_{xy_1} = 0$ where z is the distance of any point on the middle surface of a plate element from the neutral axis and W_1 is the lateral displacement in the overall buckling

mode. The mixed second order strain field is described by the following equations (Sridharan and Ali, 1985):

$$\varepsilon_{x_{12}} = u_{12,x}; \qquad \varepsilon_{y_{12}} = v_{12,y}; \qquad \text{and} \qquad \gamma_{xy_{12}} = u_{12,y} + v_{12,x}. \tag{5a–c}$$

With these stipulations, the governing equations of the mixed second order field can be expressed in the form of three partial differential equations in terms of u_{12}, v_{12} and w_{12}. These are

$$u_{12,xx} + \tfrac{1}{2}(1-v)u_{12,yy} + \tfrac{1}{2}(1+v)v_{12,xy} = 0$$

$$v_{12,yy} + \tfrac{1}{2}(1-v)v_{12,xx} + \tfrac{1}{2}(1+v)u_{12,xy} = 0$$

$$D\nabla^4 w_{12} + \sigma t w_{12,xx} = c W_{1,xx}\{z\bar{w}_2(y)\} \sin\left(\frac{m\pi x}{l}\right) \tag{6a–c}$$

where t is the thickness of the plate element, $D = Et^3/12(1-v^2)$ and $c = -Et(m^2\pi^2/l^2)$. A subscript denotes differentiation with respect to the appropriate coordinate. These equations are of the same type as those of a plate element carrying a lateral load proportional to $W_{1,xx}z(y)\cdot\bar{w}_2(y)\cdot\sin(m\pi x/l)$. Since this term varies sinusoidally with a small wave length compared to l ($m \gg 1$) (but modulated by the slowly varying function $W_{1,xx}$), the implicit use of von Karman theory in derivation of eqn (6a–c) appears justified. Since the inplane and out of plane displacements are decoupled, we may take $u_{12} = v_{12} = 0$. σ in the left hand side is the uniform stress carried by the plate structure.

Now, the term $W_{1,xx}$ may be expanded in the form of a half-range cosine series, so that,

$$W_{1,xx} = \frac{q_0}{2} + \sum q_n \cos(n\pi x/l) \qquad (n = 1, 2, \ldots) \tag{7}$$

where

$$q_n = \frac{2}{l} \int_0^l W_{1,xx} \cos(n\pi x/l) \, dx \qquad (n = 0, 1, 2, \ldots).$$

Equation (6c) may then be written as

$$D\nabla^4 w_{12} + \sigma t w_{12,xx} = \sum_n c \frac{q_n}{2} \{z\bar{w}_2(y)\} \left\{ \sin(m+n)\frac{\pi x}{l} + \sin(m-n)\frac{\pi x}{l} \right\}$$

$$= \sum_i C_i \{z\bar{w}_2(y)\} \sin\left(\frac{i\pi x}{l}\right) \tag{8}$$

where C_i is an appropriate constant.

A solution for w_{12} may be constructed as a linear combination of

(i) all the buckling modes of the plate structure of the same wave length as w_2, but orthogonal to w_2, i.e. satisfying the condition

$$\int_A \bar{w}_2(y)\bar{w}_n(y) \, dA = 0 \qquad (n \neq 2) \tag{9}$$

where the integral is taken all over the cross-sectional area, A; and

(ii) all the buckling modes composed of n ($n = 1, 2, \ldots, n \neq m$) half-waves which are orthogonal to w_2 by virtue of the equality

$$\int_0^l \sin\left(\frac{n\pi x}{l}\right) \sin\left(\frac{m\pi x}{l}\right) dx = 0 \qquad (m \neq n).$$

The orthogonality condition mentioned above is to ensure that w_{12} takes the form of only a "modification" to the participating modes (13). Thus w_{12} may be written in the form:

$$w_{12} = +[a_{2,m-2}\bar{w}_2(y)+a_{3,m-2}\bar{w}_3(y)\ldots] \sin\left[(m-2)\frac{\pi x}{l}\right]$$

$$+[a_{2,m-1}\bar{w}_2(y)+a_{3,m-1}\bar{w}_3(y)\ldots] \sin\left[(m-1)\frac{\pi x}{l}\right]+[0+a_{3,m}\bar{w}_3(y)\ldots] \sin\left[(m)\frac{\pi x}{l}\right]$$

$$+[a_{2,m+1}\bar{w}_2(y)+a_{3,m+1}\bar{w}_3(y)\ldots] \sin\left[(m+1)\frac{\pi x}{l}\right]$$

$$+[a_{2,m+2}\bar{w}_2(y)+a_{3,m+2}\bar{w}_3(y)\ldots] \sin\left[(m+2)\frac{\pi x}{l}\right] + \ldots$$

$$= \sum_p \sum_i a_{p,i}\bar{w}_p(y) \sin\left(\frac{i\pi x}{l}\right). \tag{10}$$

In the foregoing $\bar{w}_2(y)$, $\bar{w}_3(y)$ are the cross-sectional variations of the local modes with m half-waves. These shapes are deemed to remain unchanged for small changes in m. Note once again, that the coefficient $a_{2,m}$ is conspicuous by its absence. This is simply the consequence of the requirement that the higher order fields must be orthogonal to the lowest order field, i.e. the buckling mode (Budiansky, 1974).

Substituting for w_{12} from (10) into (8), multiplying both sides by $\bar{w}_p(y)$ and integrating over the cross-sectional profile, an expression for a typical coefficient in (10) may be obtained. Thus,

$$a_{p,i} = C_i \frac{\displaystyle\int_A z(y)\bar{w}_2(y)\bar{w}_p(y)\, dA}{\displaystyle\int_A L_i(\bar{w}_p(y))\bar{w}_p(y)\, dA} \tag{11}$$

where L_i is the linear differential operator given by

$$L_i(f) = D[f''' - 2i^2\pi^2 f''/l^2 + i^4\pi^4/l^4 f] - \sigma t\left(\frac{i^2\pi^2}{l^2}\right)f \tag{12}$$

where $f = f(y)$.

A major weakness in the procedure outlined above for the determination of the mixed second order field is that the term in the denominator in (11) would become zero for several modes as σ increases beyond σ_2. Even if we let $\sigma = \sigma_2$ in the evaluation of the field, the value of the denominator term in (11) may be too close to zero for comfort, especially for modes having half-waves numbering $m-2$, $m-1$, m, $m+1$, $m+2$, ... for large values of m. The solution, then, is strongly governed by the zeros of the denominator of (11). Note this is a reflection not on the real behavior, but simply the way the problem is posed and solved for.

The only way out of this difficulty is to name the modes for which the critical stress is in the proximity of σ_2, as the participating modes in the interaction. Since w_{12} must be orthogonal to all such modes, the near zero terms in the denominator in (11) do not occur any more. Also, because these modes are treated as fundamental modes, the higher order

stresses and strains associated with them are, of necessity, duly accounted for in the analysis making for a realistic appreciation of their role.

For large values of m, the number of modes (N) that are important, together with the number of associated second order fields may be so large as to introduce an unacceptable level of computational complexity which may very well blur the clear perception of mechanics of the phenomenon. The major virtues of the asymptotic method of analysis would, then, seem to be at an end. The technique of amplitude modulation is designed precisely to circumvent these difficulties. However, once introduced it takes away the strictly "asymptotic" character of the solution.

Considering eqn (6c) once again, we may treat $W_{1,xx}$ as a slowly varying function in the sense of Koiter and Pignataro (1974). The equation, then, admits of a solution in the form of a linear combination of local modes, each having the same half-wave length as the primary mode, with their amplitudes suitably modulated. Specifically, the solution for w_{12} may be sought in the form:

$$w_{12} = [a_2 f_2(x) \cdot \bar{w}_2(y) + a_3 f_3(x) \cdot \bar{w}_3(y) + \ldots] \sin \ (m\pi x/l) \tag{13}$$

where orthogonality with respect to the primary mode is still preserved by taking

$$f_2(x) = W_{1,xx} - \bar{W}_1 \ ; \qquad f_3(x) = f_4(x) = \ldots = W_{1,xx} \tag{14}$$

where $\bar{W}_1$ is the averaged value of $W_{1,xx}$ over the range 0 to l, so that

$$\int_0^l f_2(x) \ \mathrm{d}x = 0. \tag{15}$$

The constants a_i in eqn (13) may be obtained from

$$a_i = \frac{c}{\bar{J}_i} \left\{ \int_0^l W_{1,xx} f_i(x) \ \mathrm{d}x \right\} \frac{\int_A z \bar{w}_2(y) \bar{w}_i(y) \ \mathrm{d}A}{\int_A L_p(\bar{w}_i) \bar{w}_i(y) \ \mathrm{d}A} \ (i \neq 2) \tag{16}$$

where

$$\bar{J}_i = \int_0^l f_i(x) \ \mathrm{d}x.$$

The form of the expression for a_i in (16) is the direct consequence of the concept of a slowly varying function. Note that it cannot be used to evaluate a_2 as the denominator vanishes in this case. *This shows that an asymptotic approach and the concept of "slowly varying amplitude" are not compatible, so much so, one must take recourse to a nonlinear analysis of the problem* starting with unknown modulating functions associated with each mode (Koiter and Pignataro, 1976b; Sridharan and Ali, 1985). Further, any mode which gives rise to a near-singularity in eqn (16) must be incorporated as a participating mode in the analysis.

Equations (10) and (13) give alternative forms of solution to the mixed second order field. *Thus it is seen that the use of a modulating function $f_i(x)$ is substantially equivalent to taking into account the triggering of local modes of the same transverse description as $\bar{w}_i(y)$, but of slightly differing wave lengths.*

Selection of the secondary mode and the computation of w_{12}-field

It follows from the foregoing discussion that the mixed second order field (w_{12}) which arises by the interaction of the overall mode with the primary local mode, contains all the essential modes triggered by interaction, to the first order approximation. Making a fresh
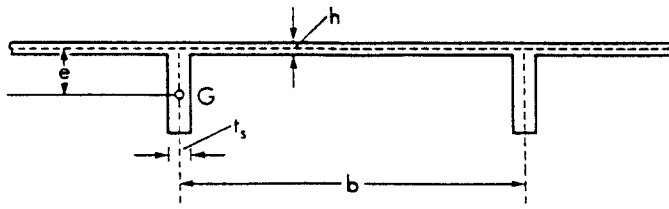
Fig. 2. The stiffened panel geometry (G = centroid of stiffener).

start with the amplitude modulated primary local mode, it is readily seen from an equation similar to (6c) that the mixed second order field has the same wave length as the primary local mode, modulated by the function $f_2(x)W_{1,cr}$. The point of interest now is the composition of the transverse variation of this field, $\bar{w}_{12}(y)$, in terms of higher local modes.

The mixed second order field may be obtained by rendering a certain potential function stationary (Benito and Sridharan, 1985). Thus, using finite strip technique, a set of linear nonhomogeneous simultaneous equations is obtained. Using the orthogonality of the buckling modes, it is a simple task to obtain the contributions of each of the modes. The procedure is briefly summarized in Appendix A.

As an illustration, we consider stiffened plates of the type shown in Fig. 2. The details of the panels investigated are given in Table 1. The first three columns thereof specify a set of parameters $(l/b, e/b, h_0)$ defining a family of panels. h_0 is the averaged thickness of the panel given by $h_0 = h + 2\,et_s/b$, the area of the stiffened plate per unit width. A member of each family identified by h/h_0 is investigated for the composition of the w_{12} field. Figure 3 (a–c) gives the shapes of the first three nontrivial modes in the ascending order of the associated eigenvalues. Each of the modes are normalized such that,

$$\int_A \bar{w}_n(y)\bar{w}_p(y)\,dA = \delta_{np}.$$

Table 2 gives the eigenvalues (critical stresses, σ_{cr}) of the modes for the three cases. Figure 4(a–c) gives the relative contributions of respective modes to the w_{12} field. It turns out that modes symmetric with respect to the stiffener have no contribution to the w_{12} field. The modes that do have significant contribution are those which tend to accentuate the deflections on one side of the axis of bending and diminish the same on the other. If $\sigma_2 < \sigma_1$, or if there be local imperfections, local buckling will occur first and, because of the asymmetry of the section, the structure will bend in the overall sense under a load whose resultant passes through the geometric centroid of the cross-section. Under this condition, the local mode will get modified and the recognition of the secondary local mode(s) is necessary to model this behavior. The effect is especially important for panels with relatively deep stiffeners in the range $\sigma_2 < \sigma_1$. These effects are contained in the mixed second order field.

Once the contributions of each of the higher modes is known, one or more of these modes, depending upon the proximity of the eigenvalues to σ_2 and their relative contribution to the $\bar{w}_{12}(y)$ field, may be chosen to be the fundamental participating modes in the interaction (in addition to the primary local mode). In the present work, we include a single non-trivial secondary local mode whose eigenvalue is closest to σ_2. The remainder of $\bar{w}_{12}(y)$ (after excluding the contribution of those modes) associated with the appropriate

Table 1. Geometric parameters of the panels

Family No.	l/b†	e/b	h_0‡	Case No.	h/h_0
1	4.0	0.05		1	0.688
2	8.0	0.10	1.454	2	0.400
3	12.0	0.15		3	0.250

† l = 454.4 for all the panels.
‡ $h_0 = h + 2et_s/b$.

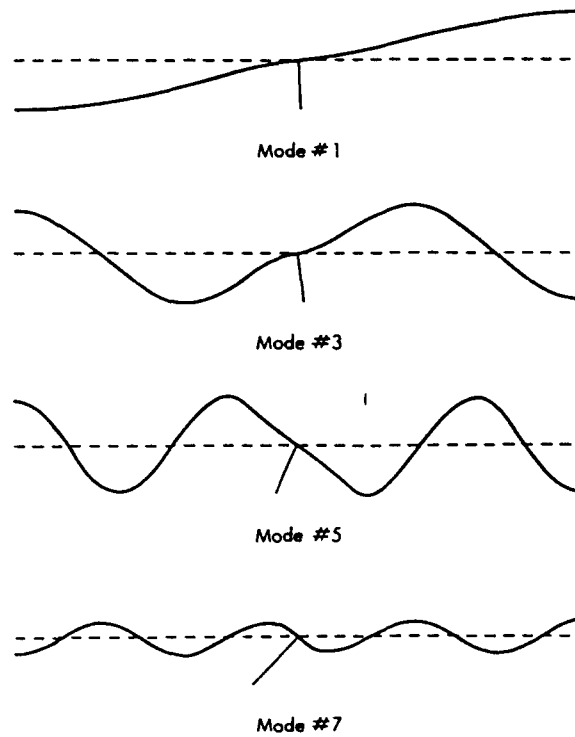Mode # 1

Mode #3

Mode #5

Mode #7

Fig. 3. The primary local mode and the first three nontrivial secondary modes of the Tvergaard panel (case 1, Table 1).

modulating function (*vide* Appendix A) constitutes the mixed second order field, w_{12}. A more direct approach to the evaluation of $\bar{w}_{12}$ would, simply, be to render the potential function (Appendix A) stationary while at the same time imposing the orthogonality conditions with respect to the chosen local modes using the Lagrange multiplier technique (Benito and Sridharan, 1985).

Beam element formulation

As explained earlier, a nonlinear analysis is called for, in order to determine the modulating functions associated with the participating local modes of buckling. This analysis is performed using beam elements in which, in addition, the lateral displacement profile of the structure is given freedom to vary as loading proceeds. Thus, in further treatment, we shall no longer be concerned with the overall buckling mode W_1, but simply with W, the lateral displacement.

The beam element, formulated in this study, has two nodes; the modulating function for each of the local mode amplitudes is linear, whereas the overall displacements, axial (U) and lateral (W), are both represented by cubic polynomials. The displacement functions

Table 2. Values of $\sigma_{cr}/E \times 10^3$ for the various modes

Case No.	1†	2‡	3§	4‡	Mode No. 5	6‡	7	8‡	9	10‡
1	0.4753	0.4883	5.937	6.230	30.03	32.41	70.45	106.1	114.6	267.1
2	0.6588	0.6611	8.381	8.435	43.25	43.88	69.69	143.7	144.1	361.5
3	0.5802	0.5809	7.395	7.411	38.38	38.55	57.89	126.1	126.2	317.5

† The primary local mode with critical stress σ_2.
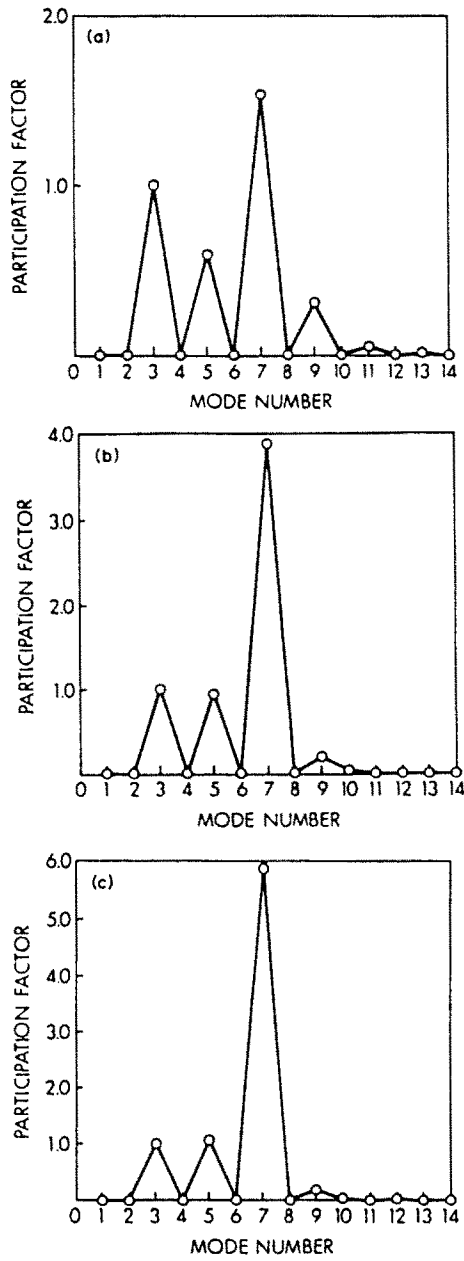‡ Modes symmetric w.r.t. to the stiffeners.
§ The secondary local mode.

Fig. 4. Relative mode participation factors for the local modes in the mixed second order field, for (a) case 1, Table 1. [Note $w_{12} = C\{b_i\bar{w}_i(y) \sin (n\pi x/l)\}$ with $b_1 = 1.0$]; (b) case 2, Table 1; (c) case 3, Table 1.

take the form

$$\xi_n = \xi_{np}\psi_p(x) \qquad (p = 1, 2) \tag{17}$$

$$U = U_i\phi_i(x)$$

$$W = W_i\phi_i(x) \qquad (i = 1, 4) \tag{18a,b}$$

where

$$\psi_1 = 1 - \eta, \qquad \psi_2 = \eta$$

$$\phi_1 = (1 - 3\eta^2 + 2\eta^3), \qquad \phi_2 = l_e(\eta - 2\eta^2 + \eta^3)$$

$$\phi_3 = (3\eta^2 - 2\eta^3), \qquad \phi_4 = l_e(-\eta^2 + \eta^3) \tag{19a-f}$$

with $\eta = x/l_e$, l_e being the length of the element and x the local axial coordinate of the element, measured from node 1.

The ξ_{n1} and ξ_{n2} represent the magnitudes of the amplitudes of the nth local mode at the nodes 1 and 2, respectively; $U_1 \ldots W_4$ are the degrees of freedom comprising of the nodal displacements and their gradients. The functions ψ and ϕ are assumed to be "slowly varying" in the sense of Koiter and Pignataro (1976a,b)—an assumption which facilitates the setting up of the potential energy function.

Energy function

The potential energy function of an element, for the perfect structure corresponding to a prescribed compressive load, P, can be expressed in the form

$$\Pi = (a_{\alpha\beta} - \sigma b_{\alpha\beta})\xi_{n\alpha}\xi_{n\beta} + (A_{ij} - \sigma B_{ij})W_iW_j + C_{ij}U_iU_j$$

$$+ \xi_{n\alpha}\xi_{p\beta}\{a_{inp\alpha\beta}U_i + b_{inp\alpha\beta}W_i + [C_{ijnp\alpha\beta}W_iW_j]\} + a_{\alpha\beta\gamma\delta npqr}\xi_{n\alpha}\xi_{p\beta}\xi_{qr}\xi_{r\delta}$$

$$+ [C_{ijk}U_iW_jW_k + D_{ijkl}W_iW_jW_kW_l] + \pi^{(1,2)} \quad (20)$$

$$\alpha,\beta,\gamma,\delta = 1,2 \qquad i,j,k,l = 1,\ldots,4 \qquad n,p,q,r = 2,\ldots,N+1$$

where $\sigma = P/A$ and $n,\ldots,r$ identify the local modes. The last term gives the contribution of the mixed second order field, detailed in Appendix A. Key steps in the derivation are given in Appendix B where the case of prescribed end compression is also considered. If U is looked upon as a sum of contributions due to local ($U^{(1)}$) and overall buckling ($U^{(2)}$), respectively, certain simplifications arise by virtue of the inextensionality of overall buckling for isolated columns. In effect, all the terms inside the square brackets vanish if we set $U = U^{(1)}$ in eqn (20). Initial imperfections can be incorporated readily in the energy expression. Again these aspects are discussed in Appendix B.

RESULTS AND DISCUSSION

Comparison with Koiter's results

Case 1 in Table 1 is the so called Tvergaard panel—a case of coincident buckling as per a rigorous calculation of σ_1 (3) and near coincident buckling ($\sigma_1/\sigma_2 = 1.02$) on the basis of a calculation as an Euler column. The panel has been analyzed by Koiter and Pignataro (1976a,b) and Tvergaard (1973). In the present study the problem is solved using 24 strips using shape functions given in Graves-Smith and Sridharan (1978) for local buckling and 10 beam elements in the interactive buckling analysis. Experience has indicated that this level of discretization is adequate for producing σ_u within a tolerance limit of 0.01%. The stresses were summed up at the ends and produced values which were exactly equal to the applied load.

Case 1 : simply supported panel. The sensitivity to local imperfection of this panel is first investigated with the overall imperfection set to zero. To facilitate comparison with Koiter's work, only the primary local mode is considered in the analysis. Note that imperfections are given by ξ_1^0 and ξ_2^0, which are the appropriate magnitudes divided by h. It is seen that for the smaller values of the local imperfections the curves have well defined limit points; and for the larger values the peak disappears and all the characteristics approach asymptotically the same value of load as deflections increase (not illustrated). These observations agree well with the earlier findings of Koiter and Pignataro (1976b). Figure 5(a) shows a comparison of the variation of the maximum load (as given by σ_u/σ_2) carrying capacity with local imperfection magnitudes as obtained by Koiter and Pignataro (1976b) and the present theory. Agreement is seen to be excellent. For the panel, Koiter predicted a lower bound of the maximum load carrying capacity given by $\sigma_u/\sigma_2 = 0.889$—a prediction which seems to be well borne out by the results of the present study. Figure 5(b) shows the nondimensional load–end shortening relationships for the panel with various levels of initial overall imperfections. Koiter *et al.* obtained a value of $0.95\sigma_2$ for the value of the average
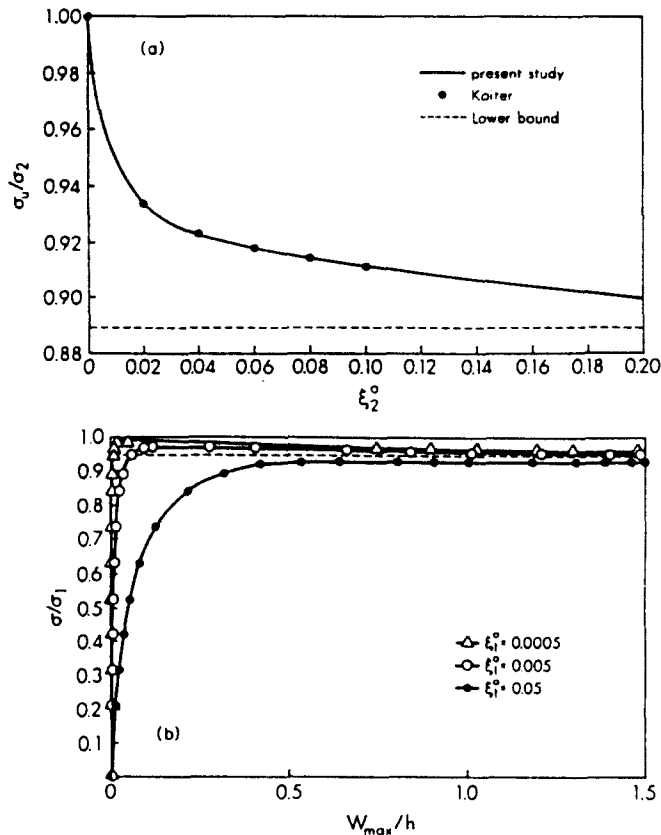
Fig. 5. (a) Sensitivity to local imperfection of Tvergaard panel—a comparison with Tvergaard (1973a). $\bar{\xi}_2$ is the amplitude of the imperfection in the form of local mode normalized with respect to h. (b) Nondimensional load deflection relations as the overall imperfection $\bar{\xi}_1$ is varied. (A constant local imperfection $\bar{\xi}_2 = 0.001$ is assumed in all the cases.)

stress as the one to which all the characteristics will approach [the dashed line in Fig. 5(b)]. This observation is borne out by the present study. However, the present study indicates marginally smaller imperfection-sensitivity than predicted by Koiter *et al*. This is evidenced by the fact that the characteristic for the case $\bar{\xi}_1 = 0.005$, rises above the value 0.95 before it descends whereas Koiter's theory indicates that it would never rise above 0.95 but approach it asymptotically. The discrepancy must be attributed to Koiter's "lower bound approach" to the local buckling deformation which tends to exaggerate the effects of the interaction.

Case 2: multibay panel. An example of a multibay panel was studied for comparison with Koiter's work. The panel has two equal spans and is continuous over an intermediate support with simply supported ends. It is observed that the imperfection-sensitivity as given by the present model is once again less severe compared to that reported by Koiter. For the case of multibay Tvergaard panel with $\xi_1^0 = 0.005$, σ_u as given by the present theory is $0.98\sigma_1$ (where σ_1 is the Euler critical stress) in contrast to $0.96\sigma_1$ reported by Koiter and Pignataro (1976b).

The detailed nonlinear analysis performed in the present study reveals some interesting features not discussed by Koiter. Figure 6(a,b) gives the *x*-variation of local buckling amplitude ξ_2 and the overall deflection W, respectively, for a panel with imperfections $\xi_1^0 = 0.005$ (in the form of a two-half-wave sine mode) and $\xi_2^0 = 0.1$, a constant. For $\sigma \ll \sigma_1$, the amplitude of local buckling is substantially uniform and the overall deflections are greater in the left spans where the plate is subjected to additional compression due to bending. As $\sigma \to \sigma_1$, the panel bends in the two-half-wave sine mode, but local buckling deflections are concentrated on the left span only. This illustrates the important role
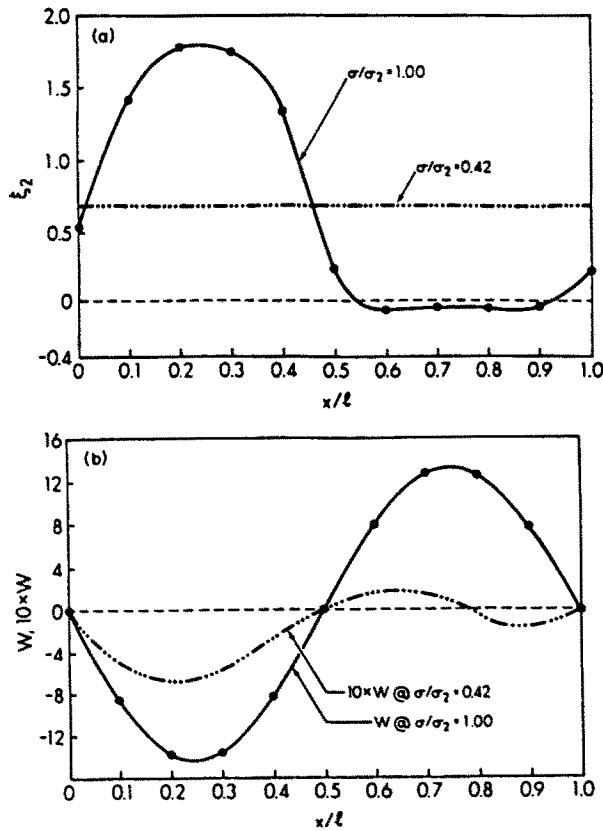
Fig. 6. (a) The variation of local buckling amplitude along the length of a two span continuous Tvergaard panel ($\xi_1^0 = 0.005$, $\xi_2^0 = 0.1$). The initial overall imperfection is assumed in the form of two half sine waves. (b) The variation of overall deflection along the length of the multibay panel ($\xi_1^0 = 0.005$, $\xi_2^0 = 0.1$).

performed by the asymmetry of the section in controlling the variation of the modulating function in multibay panels.

Comparison with Tvergaard's results

We next compare the maximum capacities of panels as given by Tvergaard and the present theory. The key geometric parameters of three families of panels are already listed in Table 1. Families 1 and 2 have been studied by Tvergaard (1973b), for three levels of initial imperfections, given by ξ_1, ξ_2 which are the imperfection amplitudes divided by h_0. Note in all the three cases $\xi_1 = \xi_2$. As shown in Table 1, h_0 and l, are both kept constant for all the three families of panels identified by the values of l/b and e/b. For each family, the plate thickness h is systematically varied and this provides a simple means of apprehending the optimal distribution of material between the plate and the stiffener.

Figure 7(a,b) gives the variation of the maximum carrying capacity (σ_u) with h/h_0 for panels of family 1 and 2 as obtained by Tvergaard and the present theory and represented by continuous and dashed lines, respectively. Note that the capacity is expressed in a dimensionless form by dividing it by σ_0 given by

$$\sigma_0 = \frac{E\pi^2}{12}\left(\frac{h_0}{b}\right)^2,$$

the overall critical stress in the absence of a stiffener. The figure also gives the overall and primary local critical stresses in appropriate dimensionless forms.

It is seen that there exists close agreement between the sets of results. For case 1 [Fig. 7(a)], the results produced by Tvergaard are consistently lower and this is attributable
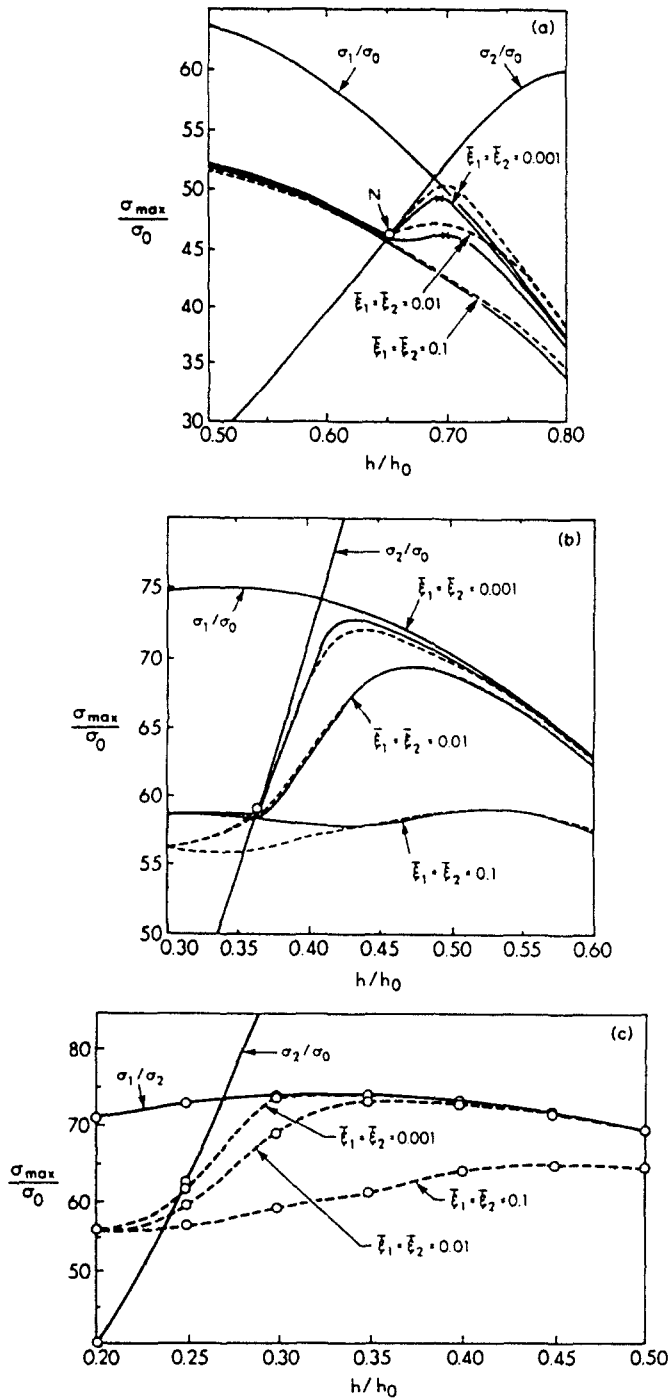
Fig. 7. (a) The variation of the maximum local carrying capacity of the panel designated as Family 1, Table 1, with h/h_0 for three levels of initial imperfections indicated. $\zeta_1 = \zeta_2$. ζ_1 and ζ_2 are initial imperfections divided by h_0. (σ_1 is the "exact" overall critical stress.) (b) The variation of the maximum local carrying capacity of the panel designated as Family 2, Table 1, with h/h_0 for three levels of initial imperfections. (σ_1 is the "exact" overall critical stress.) (c) The variation of the maximum local carrying capacity of the panel designated as Family 3, Table 1, with h/h_0 for three levels of initial imperfections. (σ_1 is the Euler critical stress.)

to the more accurate calculation of the overall buckling stress by Tvergaard which accounts for shear lag effects and cross-sectional distortions together with the associated second order effects. On the whole, the two results are within 3% of each other and considering the differences in the calculation procedure, this is not surprising. For case 2 [Fig. 7(b)]. the results given by the present theory are somewhat lower for panels with $\sigma_2 < \sigma_1$ and for
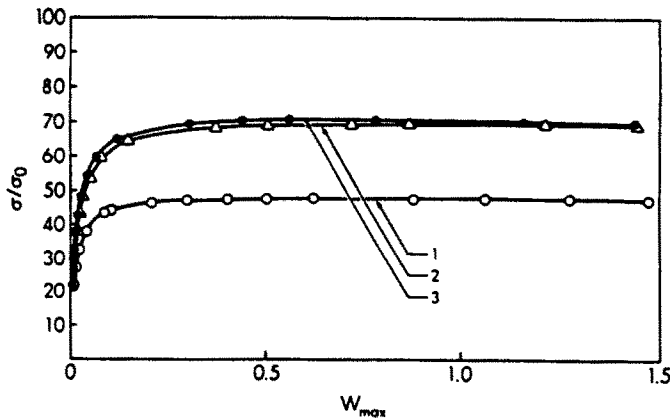
Fig. 8. The non-dimensional load–deflection relationships of optimal panels of each of the families
($\zeta_1 = \zeta_2 = 0.01$); W_{max} is maximum value of W.

higher levels of imperfections. This is believed to be due to the more accurate treatment of local buckling in terms of amplitude modulation in the present work.

Optimality of the design

Figure 7(a–c) gives the variation of the maximum carrying capacity of the panels for the three families of panels listed in Table 1, for three different levels of imperfections. In all the three cases, there are two regions of high values of σ_u/σ_0, each located on either side of the naive optimum ($\sigma_1/\sigma_2 = 1$). On the left hand side, ($\sigma_1/\sigma_2 > 1$), the maximum capacity is reached after considerable local buckling and the loss of stiffness, whereas on the right side ($\sigma_1/\sigma_2 < 1$), it occurs with little loss of stiffness (Fig. 8). The latter optimum is clearly preferable when both the stiffness and the strength considerations are taken together. The optimum value of σ_1/σ_2 shifts downward from unity and the shift increases with initial imperfections. These observations confirm the earlier findings of Tvergaard (1973b). The results also indicate that the shift from the naive optimum increases as well with e/b— something which prevents the stiffener being made too stocky at the expense of the plate. For Family 3 with the deepest stiffeners [Fig. 7(c)], the ratio σ_1/σ_2 for optimal panel is as low as 0.40 with imperfections given by $\zeta_1 = \zeta_2 = 0.1$. An interesting feature of this case is that the σ_u/σ_0 is only about 90% of the naive optimum value, but the sensitivity to the imperfections of the optimal design is minimal.

In order to check the stiffness characteristics of the optimal solutions the load deflection characteristics are plotted for each case taking $\zeta_1 = \zeta_2 = 0.01$ (Fig. 8). It appears that all the panels retain much of their stiffness in the unloading process and would perform well in a displacement-controlled loading.

Comparison with experimental results of Thompson et al.

A detailed experimental study on stiffened panels was undertaken by Thompson et al. (1974). A series of small scale specimens was fabricated from epoxy plastic—a material which remains linearly elastic over a considerable range of strain. From a description of the experimental procedure, it appears that a high degree of control was exercised in fabricating the specimens to prescribed levels of initial imperfections and testing them. Thus, these test results are probably of considerable value from the point of view of validation of the elastic theories of mode interaction in stiffened panels.

The test specimens were of two types:

(i) stiffened plates having eight bays and carrying stocky stiffeners;
(ii) stiffened plates having nine bays and carrying slender stiffeners.

Table 3.

Stiffener type	h	Dimensions (mm)			No. of bays
		b	t_s	$d = (2e)$	
"Stocky"	0.75	57.5	4.90	9.625	8
"Thin"	0.75	46.5	0.75	14.025	9

Table 3 summarizes the details of the test specimens. Thompson *et al.* define the local critical loads as

$$P_L = AkE\pi^2 h^2 / \{12(1 - v^2)b^2\}$$

where A is the total cross-sectional area and k the buckling coefficient. In cases (i) and (ii), the value of k was taken as 6.986 and 4.0, respectively, to correspond with clamped and simply supported end conditions of the panel. With these values of P_L, the length of the plate used in the experiments could be arrived at for any given ratio of P_L to the Euler critical load P_E. In the present study, of course, local critical loads and modes were obtained rigorously using finite strips on an isolated panel. In the treatment of overall buckling, the position of the neutral axis of the isolated panel was taken to be the same as that of the full stiffened plate, to reflect the presence of an extra stiffener compared to the number of bays.

Figure 9(a–c) plots the experimental and theoretical results against each other. The agreement appears to be extremely good indeed. However, in order to achieve this result, some fine tuning of the model was necessary. In the case of specimens with $P_L/P_E = 0.64$ and possessing relatively high levels of overall imperfection ($\xi_2^0 = w_0/h > 0.5$), collapse was characterized by the deflections taking on huge values as the load increases at an extremely slow rate. With deflections approaching 2–3% of the span, it was clear the overall curvature χ could no longer be accurately represented by $W_{1,xx}$. This simplified formula results in an underestimate of the key destabilizing term given by the product of $z\chi$ with $\frac{1}{2}w_{2,x}^2$ in the expansion

$$\varepsilon_x^2 = \{-z\chi + \tfrac{1}{2}w_{2,x}^2 + \ldots\}^2.$$

In order to improve the accuracy of this important term, the curvature was represented more accurately by the expression

$$\chi = W_{,xx}\{1 + \tfrac{1}{2}W_{,x}^2\}$$

which is the result of truncation of the series representation of the exact beam curvature formula (Thompson and Hunt, 1973),

$$\chi = W_{,xx}/\{1 - W_{,x}^2\}^{1/2}.$$

Inclusion of this term can make a difference of 2–3% besides giving a maximum in the load deflection characteristic thus obviating the need to estimate the asymptotic value of load as deflections tend to infinity.

The case of the panel with slender stiffeners is of considerable interest as this has not been explored analytically or experimentally in any great detail. In Fig. 10(a,b) are shown the primary local mode and the associated secondary mode of the same wave-length. The magnitudes of the critical stresses are also indicated therein. The former is the usual "plate" mode and the latter is the "stiffener" mode. As long as the plate bends such that the stiffener carries the tension due to bending, the stiffener mode has a relatively small influence. For negative values of ξ_1^0, however, the additional compression is thrown on the stiffener and the stiffener mode plays a crucial role in the interaction.

In order to reflect this behavior, the local imperfections are assumed in the plate mode and stiffener mode respectively for positive and negative values of overall imperfections.
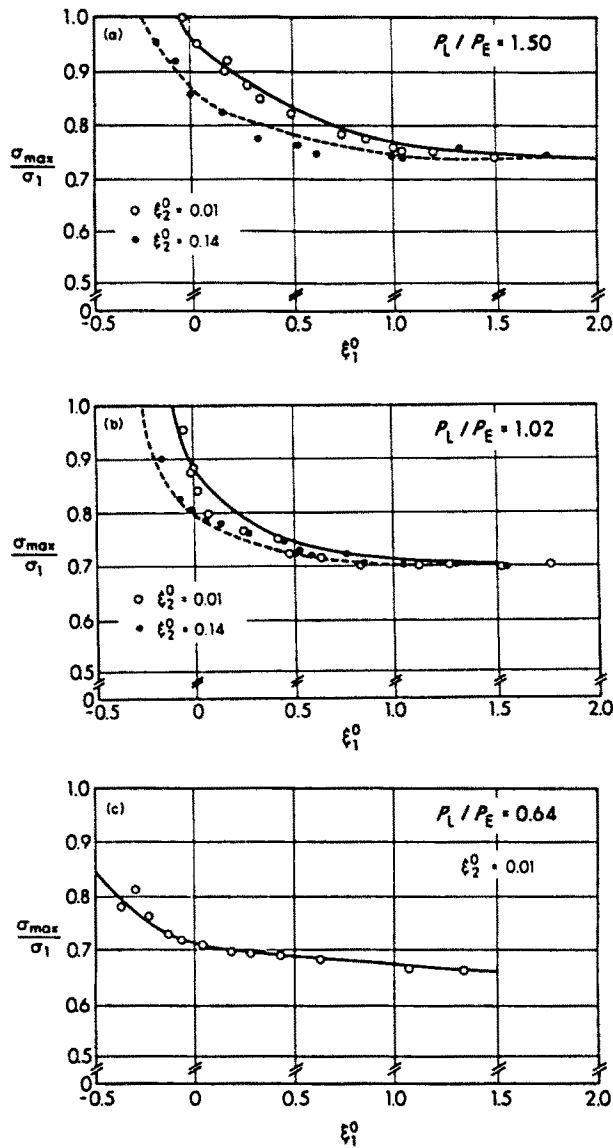
Fig. 9. Comparison of theoretical and experimental results of Thompson *et al.* (1976) for panels with stocky stiffeners. (a) $P_L/P_E = 1.50$, $l = 372$ mm, $m = 10$. The continuous and dashed lines represent the theoretical results for $\xi_2^0 = 0.01$ and 0.14, respectively. (b) $P_L/P_E = 1.02$, $l = 307$ mm, $m = 8$. The continuous and dashed lines represent the theoretical results for $\xi_2^0 = 0.01$ and 0.14, respectively. (c) $P_L/P_E = 0.64$, $l = 243$ mm, $m = 6$. The continuous line represents the theoretical results.

(Introduction of imperfections in any one mode would, however, automatically trigger the other because of nonlinear interactive terms present in the potential energy function.) Thompson *et al.* report the magnitudes of imperfections in the panel and do not mention the imperfections that may be present in the stiffeners. Thus, in both the cases, the magnitudes of plate imperfections at the middle of the bay were taken as w_0 as reported in Thompson *et al.* (1976). This probably exaggerated the stiffener imperfections to a certain extent, when the imperfections were assumed in the stiffener mode.

Figure 11 shows the comparison of the experimental and theoretical results of panels with slender stiffeners.

On the right hand side, the two results are in very good agreement for the smaller level of local imperfection, *viz.* $w_0/h = 0.02$. For the higher level of local imperfections, the results do not show such a precise agreement. It is not obvious why this discrepancy arises, even though it is easy to speculate on it. One key observation is that experimental values
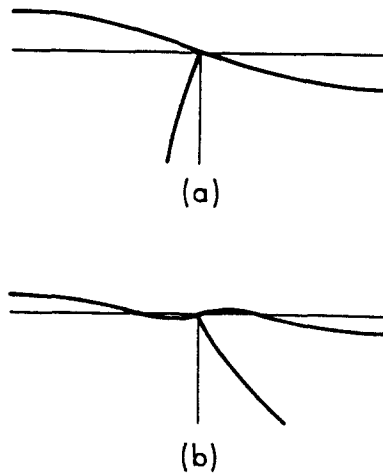
Fig. 10. Local buckling modes of panel with thin stiffeners. (a) "Plate mode" $(\sigma_2/E = 0.992 \times 10^{-3})$;
(b) "stiffener mode" $(\sigma_3/E = 0.441 \times 10^{-3})$.

of maximum load do not vary with imperfections for $\xi_1^0 > 0.25$—an unlikely scenario for the case of near-coincident buckling. Evidently, there is some scatter due to minor experimental errors in this region. In any case, the maximum discrepancy is less than 10% and need not, perhaps, cause much concern.

On the left hand side, the agreement is, once again, very satisfactory for smaller magnitudes of local imperfection, but for the case $w_0/h = 0.1$, the theoretical results tend to be lower. This is believed to be due to the exaggeration of stiffener imperfections mentioned earlier.

CONCLUSIONS

A new analytical model for stiffened panels is described. The phenomenon of amplitude modulation and the triggering of the secondary mode are shown to be the logical consequences of the interaction of overall bending with the primary local mode.

The results given by the model compare well with those given by Koiter and Pignataro (1976a,b) and Tvergaard (1973b) for the case of panels with stocky stiffeners. The theory also compares favorably with experimental results obtained by Thompson et al. (1974) for cases of panels with stocky and slender stiffeners. The latter case is one of interaction of overall mode with "panel" and "stiffener" local modes.

For panels with imperfections, the optimum design shifts to the range $\sigma_1/\sigma_2 < 1$. This conclusion is in agreement with the earlier finding of Tvergaard. Assuming nominal, but minimal imperfections, it is found that an optimally designed panel retains much of its (secant) stiffness in the unloading process; and as long as no material damage occurs, no catastrophic failure is expected.
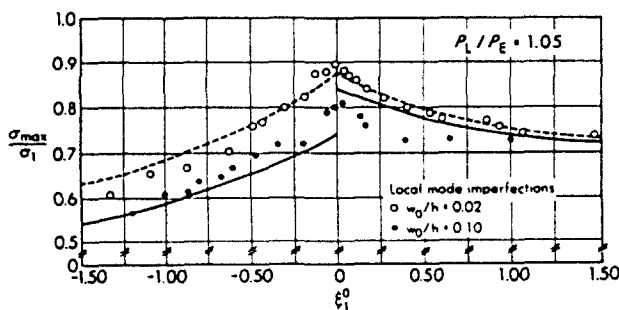

Fig. 11. Comparison of theoretical and experimental results for panel with thin stiffeners in Thompson et al. (1974) $(P_L/P_E = 1.05, l = 395$ mm, $m = 8)$. The dashed and continuous lines represent the theoretical results for $w_0/h = 0.02$ and 0.10, respectively.

REFERENCES

Ali, M. A. and Sridharan, S. (1988). A versatile model for interactive buckling of columns and beam-columns. *Int. J. Solids Structures* 24, 481–496.

Benito, R. and Sridharan, S. (1985). Interactive buckling analysis with finite strips. *Int. J. Numer. Meth. Engng* 21, 145–161.

Benthem, J. P. (1959). The reduction in stiffness of combinations of rectangular plates in compression after exceeding the buckling load. NLL-TR S.539.

Budiansky, B. (1974). Theory of buckling and postbuckling behavior of elastic structures. In *Advances of Applied Mechanics* (Edited by C. S. Yih), Vol. 14, pp. 1–66. Academic Press, New York.

Graves-Smith, T. R. and Sridharan, S. (1978) A finite strip method for the post-locally buckled analysis of plate structures. *Int. J. Mech. Sci.* 20, 833–842.

Koiter, W. T. and van der Neut, A. (1980). Interaction between local and overall buckling of stiffened compression panels. In *Thinwalled Structures* (Edited by J. Rhodes and A. C. Walker), pp. 61–85. Granada, London.

Koiter, W. T. and Pignataro, M. (1976a). An alternative approach to the interaction between local and overall buckling in stiffened panels. In IUTAM Symposium, Cambridge, MA, 1974, *Buckling of Structures* (Edited by B. Budiansky), pp. 133–148. Springer, Berlin.

Koiter, W. T. and Pignataro, M. (1976b). A general theory for the interaction between local and overall buckling in stiffened panels. Delft University of Technology, Dept. of Mechanical Engineering, Report WTHD-83.

van der Neut, A. (1976). Mode interaction in stiffened panels. In IUTAM Symposium, Cambridge, MA, 1974, *Buckling of Structures* (Edited by B. Budiansky), pp. 117–132. Springer, Berlin.

Sridharan, S. (1982). A finite strip analysis of locally buckled plate structures subject to nonuniform compression. *Engng Struct.* 4, 249–255.

Sridharan, S. and Ali, M. A. (1985). Interactive buckling in thin-walled beam columns. *J. Engng Mech., ASCE* 111, 1470–1486.

Thompson, J. M. T. and Hunt, G. W. (1973). *A General Theory of Elastic Stability.* John Wiley.

Thompson, J. M. T., Tulk, J. D. and Walker, A. C. (1976). An experimental study of imperfection-sensitivity in the interactive buckling of stiffened plates. In IUTAM Symposium, Cambridge, MA, 1974, *Buckling of Structures* (Edited by B. Budiansky), pp. 149–159. Springer, Berlin.

Tvergaard, V. (1973a). Imperfection-sensitivity of a wide integrally stiffened panel under compression. *Int. J. Solids Structures* 9, 177–192.

Tvergaard, V. (1973b). Influence of postbuckling behavior in optimum design of stiffened panels. *Int. J. Solids Structures* 9, 1519–1534.

APPENDIX A: DETERMINATION OF w_{12}-FIELD

The potential function for the determination of the w_{12}-field is a subset of the total potential energy function and consists of all the terms associated with $\xi_1^2\xi_2^2$ (ξ_1, ξ_2 are the scaling factors of the overall (No. 1) and the primary local (No. 2) modes, respectively). Thus it consists of quadratic terms in w_{12} (since w_{12} itself is proportional to $\xi_1\xi_2$) and linear terms in w_{12} but associated with a coefficient proportional $\xi_1\xi_2$. The former set of terms arises from plate bending and loss of potential of the prescribed axial compression, while the latter arises as part of energy of in-plane deformation. In order to demonstrate this, we quote here the relevant parts of the expression for in plane strain.

$$\varepsilon_x = -\frac{\sigma}{E} - zW_{1,xx} + w_{2,x}w_{12,x} + \tfrac{1}{2}w_{2,x}^2 + \ldots \tag{A1}$$

$$\varepsilon_y = \nu\left(\frac{\sigma}{E} + zW_{1,xx}\right) + w_{2,y}w_{12,y} + \tfrac{1}{2}w_{2,y}^2 + \ldots \tag{A2}$$

Substitution of these into the expression (B7) of Appendix B and collection of only the terms proportional to $W_1^2w_2^2$, yield the required potential function. Thus,

$$\pi^{(1,2)} = \frac{D}{2}\iint \{w_{12,xx}^2 + w_{12,yy}^2 + 2\nu w_{12,xx}w_{12,yy} + 2(1-\nu)w_{12,xy}^2\}\,dx\,dy - \frac{\sigma}{2}\iint w_{12,x}^2\,dx\,dy$$
$$+ Et\iint \{-zW_{1,xx}w_{2,x}w_{12,x}\}\,dx\,dy. \tag{A3}$$

Note that this expression represents fully the potential energy contribution due to w_{12}-field, as the rest of the terms arising therefrom are neglected since they are of a higher degree than the quartic. We set $\sigma = \sigma_2$ in the evaluation of (A3).

Using the finite strip technique, $\pi^{(1,2)}$ can be expressed in the form

$$\pi^{(1,2)} = \frac{1}{2!}A_{ij}w_{12_i}w_{12_j} - B_iw_{12_i}(\chi\xi_2) \tag{A4}$$

where χ ($= W_{1,xx}$) and ξ_2 are not integrated as they are unknown "slowly varying" functions (treated as if they

are constants here); A_{ij} and B_i are coefficients resulting from integration; and w_{12_i} are the degrees of freedom representing w_{12}.

The system of equations giving w_{12} takes the form

$$A_{ij}w_{12_j} = \chi \xi_2 B_i. \tag{A5}$$

Taking

$$w_{12_i} = \Sigma a_n w_i^{(n)} \tag{A6}$$

where a_n is the participating factor of the nth local mode and using the orthogonality conditions between the various buckling modes, we obtain

$$a_n = (\chi \xi_2)\frac{B_i w_i^{(n)}}{A_{ij}w_i^{(n)}w_j^{(n)}} \qquad \text{(no sum on } n\text{)}. \tag{A7}$$

In the nonlinear analysis, using beam elements, χ is the curvature given by $W_{,xx}$ and the modulating function for the w_{12}-field is $W_{,xx}\xi_2\psi$.

APPENDIX B: POTENTIAL ENERGY FUNCTION

Strain components due to local buckling only

The second order strain components at any point on the middle surface of a plate element are given by von Karman type equations such as:

$$\varepsilon_{pq} = \frac{\partial u_{pq}}{\partial x} + \frac{1}{2}\frac{\partial w_p}{\partial x}\frac{\partial w_q}{\partial x} \qquad (p,q = 1,\ldots,N) \tag{B1}$$

where a double subscript gives a second order field and a single subscript the first order field. The expressions for W_p, U_{pq}, etc. are given by eqns (1) and 2(a–c). Note that $u_{pq} \equiv u_{qp}$, $\varepsilon_{pq} \equiv \varepsilon_{qp}$, etc. Note that the second order field are obtained as if for a prescribed end shortening.

With the amplitudes modulated, the normal strain component in the axial direction $\bar{\varepsilon}_x$ associated with local buckling can be written as:

$$\bar{\varepsilon}_x = \varepsilon_{x_{pq}}\xi_{pi}\xi_{qj}\psi_i\psi_j \qquad p,q = 2,\ldots,N, \qquad i,j = 1,2 \tag{B2}$$

where ξ_{ip} gives the amplitude of the ith mode at pth node in an element. Similar expressions can be written by other strain components, viz. $\bar{\varepsilon}_y$ and $\bar{\gamma}_{xy}$.

The case of prescribed end-shortening

Let the end shortening at the centroid be Δ and $\lambda = \Delta/l$. The total axial displacement U_T may be taken in the form

$$U_T = -\lambda x + U \tag{B3}$$

where U is the axial displacement contributed by buckling. In this case, U must be prescribed to be zero at the ends of the structure in order that $U_T|_{x=l} = -\Delta$. Making use of the displacement functions in eqn (19a–f), the total strain components may be written in the form:

$$\varepsilon_x = \bar{\varepsilon}_x + [U_i\phi_i + \tfrac{1}{2}W_iW_j\phi_i'\phi_j' - zW_i\phi_i''] - \lambda$$
$$\varepsilon_y = \bar{\varepsilon}_y + v\{\lambda - [U_i\phi_i + \tfrac{1}{2}W_iW_j\phi_i'\phi_j' - zW_i\phi_i'']\}$$
$$\gamma_{xy} = \bar{\gamma}_{xy} \qquad (i,j = 1,\ldots,4). \tag{B4a–c}$$

The total potential energy reduces to that of total strain energy in this case. The linear term involving λ and U vanishes because of the said end conditions which make U vanish at the ends. The expression for the potential energy of the perfect structure may be computed from

$$\pi = \iint\left\{\varepsilon_x^2 + \varepsilon_y^2 + v\varepsilon_x\varepsilon_y + \frac{(1-v)}{2}\gamma_{xy}^2\right\}dx\,dy + \iint\{\chi_x^2 + \chi_y^2 + 2v\chi_x\chi_y + 2(1-v)\chi_{xy}^2\}dx\,dy + \pi^{(1,2)} \tag{B5}$$

where the second term gives the contribution of the bending energy associated with local buckling. The energy expression for the perfect structure takes the same form as given in eqn (20) where $E\lambda$ replaces σ.

The case of prescribed axial load

Let the prescribed load be given by $\sigma_0 = P_0/A$ where P_0 is the axial load and A the cross-sectional area. In this case it is convenient to write

$$U = U^{(1)} + U^{(2)} \tag{B6}$$

where $U^{(1)}$ and $U^{(2)}$ are, respectively, the contributions of local buckling and overall bending. All the U's vanish at $x = 0$, but none of them vanishes at $x = l$. $U^{(1)}$ and $U^{(2)}$ are given by the same functions as U. In the case of pure local buckling, $U^{(1)}$ at $x = l$ is given by

$$\Delta = -\left\{\frac{\sigma_0}{E}\right\}l + U^{(1)}\bigg|_{x=l} \tag{B7}$$

The second term gives the additional end shortening caused by local buckling in an axially compressed member. The total strain component ε_x at any point is given by

$$\varepsilon_x = \bar{\varepsilon}_x + \{U_i^{(1)}\phi_i' - zW_i\phi_i''\} - \frac{\sigma}{E} \qquad (i = 1, \ldots, 4) \tag{B8}$$

which results from the inextensionality of overall deformations given by

$$\frac{dU^{(2)}}{dx} + \frac{1}{2}\left(\frac{dW}{dx}\right)^2 = 0. \tag{B9}$$

The strain component ε_y is then given by

$$\varepsilon_y = \bar{\varepsilon}_y + v\left\{\frac{\sigma}{E} - [U_i^{(1)}\phi_i' - zW_i\phi_i'']\right\} \qquad (i = 1, \ldots, 4). \tag{B10}$$

A potential energy function may now be constructed summing the strain energy and the loss of potential of the applied load. The latter consists of two linear terms: the one involving $U^{(2)}$ is replaced by a quadratic term by virtue of eqn (B9); the other involving $U^{(1)}$ is cancelled out by an equal term of opposite sign arising from the strain energy expansion (B4). The potential energy expression takes the simplified form

$$\pi = \left[a_{pqij} - \left(\frac{\sigma}{E}\right)b_{pqij}\right]\xi_{pi}\xi_{qj} + C_{mn}U_m^{(1)}U_n^{(1)} + \left[A_{mn} - \left(\frac{\sigma}{E}\right)B_{mn}\right]W_m W_n + C_{milpq}W_m\xi_{ip}\xi_{jq}$$

$$+ d_{mpqij}U_m^{(1)}\xi_{pi}\xi_{qj} + a_{pqrijkl}\xi_{pi}\xi_{qj}\xi_{rk}\xi_{sl} + \pi^{(1,2)} \tag{B11}$$

$$p,q,r,s = 1, \ldots, N \qquad i,j,k,l = 1,2 \qquad m,n = 1, \ldots, 4.$$

Modifications due to imperfections

Let the initial imperfections in the form of pth local mode be defined by ξ_{pi}^0, the amplitude at the ith node in an element, then a typical strain component $\bar{\varepsilon}_x$ may be written in the form

$$\bar{\varepsilon}_x = \varepsilon_{x_m}\{\xi_{pi}\xi_{qj} + \xi_{pi}\xi_{qj}^0 + \xi_{pi}^0\xi_{qj}\}\psi_p\psi_q. \tag{B12}$$

The expressions ε_x and ε_y (B4a,b) are modified as

$$\varepsilon_x = \bar{\varepsilon}_x + [U_i\phi_i' + \tfrac{1}{2}(W_iW_j + 2W_iW_j^0)\phi_i'\phi_j' - zW_i\phi_i''] - \lambda$$

$$\varepsilon_y = \bar{\varepsilon}_y + v\{\lambda - [U_i\phi_i' + \tfrac{1}{2}(W_iW_j + 2W_iW_j^0)\phi_i'\phi_j' - zW_i\phi_i'']\} \tag{B13a,b}$$

where W_i^0 is related to the overall imperfection W^0 by $W^0 = W_i^0\phi_i$.

Equation (B9) is modified as:

$$\frac{dU^{(2)}}{dx} + \frac{1}{2}\left(\frac{dW}{dx}\right)^2 + \left(\frac{dW}{dx}\right)\left(\frac{dW^0}{dx}\right) = 0. \tag{B14}$$